0026-895X/94/061028-08$03.00/0

MOLECULAR PHARMACOLOGY, 46:1028–1035, 1994.

Selective Labeling and Localization of the M4 (m4) Muscarinic Receptor Subtype

GABY FERRARI-DILEO, MAGALI WAELBROECK, DEBORAH C. MASH, and DONNA D. FLYNN

Departments of Molecular and Cellular Pharmacology (G.F.-D., D.C.M., D.D.F.) and Neurology (D.C.M.), University of Miami School of Medicine, Miami, Florida 33101, and Department of Biochemistry and Nutrition, Medical School, Université Libre de Bruxelles, B-1000 Brussels, Belgium (M.W.)

Received July 8, 1994; Accepted September 19, 1994

SUMMARY

We report here a novel strategy for the selective labeling and localization of the M4 (m4) muscarinic receptor subtype, based on the distinct kinetics of the muscarinic antagonists dexetimide and *N*-methylscopolamine (NMS) and on the selectivity profile of guanylpirenzepine and AF-DX 116 for the m1–m5 muscarinic receptor subtypes expressed in CHO-K1 cells. Incubation with 10 nM dexetimide, a nonselective antagonist, resulted in >90% occupancy of each of the m1–m5 receptor subtypes. The relatively rapid rates of dexetimide dissociation from the m1, m2, and m4 receptor subtypes ($t_{½}$ values of <12.5 min) and the slower rates of dexetimide dissociation from the m3 and m5 receptor subtypes ($t_{½}$ values of 65 and 75 min, respectively) favored the labeling of the m1, m2, and m4 receptor subtypes with short incubations with [^{3}H]NMS. Inclusion of 200 nM guanylpirenzepine and 250 nM AF-DX 116 prevented the binding of [^{3}H]NMS to the majority of the m1 and m2 receptor subtypes, respectively, resulting in primary labeling of the m4 receptor subtype. Brief dissociation of the radioligand in the presence of 1 μM atropine improved the ratio of m4 to m2 labeling by selectively removing [^{3}H]NMS from the m2 subtype. Under these conditions, the ratio of [^{3}H]NMS binding to the m4 versus m1, m2, m3, and m5 receptor subtypes was 4:1. *In vitro* autoradiography combined with these m4-selective labeling conditions demonstrated that the M4 (m4) receptor subtype was localized to the primary visual area (V1, area 17, occipital cortex) and the basal ganglia, a distribution distinct from that demonstrated for the M1 (m1), M2 (m2), and M3 (m3) receptor subtypes. These results demonstrate that a combination of the distinct kinetics of dexetimide and NMS and the receptor subtype selectivity of guanylpirenzepine and AF-DX 116 provides a valuable labeling strategy to examine the distribution and localization of the M4 (m4) muscarinic receptor subtype in brain, peripheral tissues, and cell lines.

Muscarinic receptors have a multiple (seven)-transmembrane domain conformation and are coupled to heterotrimeric G proteins, which serve to translate the extracellular signal of acetylcholine binding into a secondary intracellular response (1). Five distinct muscarinic receptor subtypes have been identified, cloned, and expressed in multiple cell types. M1, M2, M3, and M4 designate the pharmacologically defined receptor subtypes, whereas m1–m5 designate the cloned receptors. Based on pharmacological criteria, M1 and M2 correspond to muscarinic receptors with high and low affinities, respectively, for the muscarinic antagonist pirenzepine (2, 3), M3 is defined by its low affinities for pirenzepine (relative to the M1 receptor subtype) and for AF-DX 116 (relative to the M2 receptor subtype) (4), and M4 is defined by its relatively higher affinity for methoctramine and himbacine, compared with the other receptor subtypes (5). Precise correlations of the pharmacology, function, and regional expression of the pharmacologically defined and molecularly defined muscarinic receptor subtypes have not been made. *In situ* hybridization studies show that mRNAs for the individual m1–m5 receptor subtypes are expressed and specifically localized in different brain regions (6–8). The M1 subtype found at high concentrations in the forebrain and telencephalic structures, the M2 subtype in heart and basal forebrain, the M3 subtype present in glands, and the M4 subtype found at high levels in caudate putamen appear to be encoded by the m1, m2, m3, and m4 receptor genes, respectively (6, 9, 10).

One of the major complications encountered in biochemical characterization and anatomical localization studies has been the lack of receptor subtype-selective ligands. Currently available muscarinic ligands demonstrate overlapping affinities, with ≤5-fold selectivity between the receptor subtypes (11, 12). Although many studies have attempted to distinguish receptor subtypes by equilibrium binding of two or more ligands, recent studies have demonstrated that a combination of kinetic and

This work was supported by grants from the National Institute of Neurological Disorders and Stroke (NS19065) and the National Institute on Drug Abuse (DA06227) of the United States Public Health Service and from the Alzheimer's Disease Research Grant Program of the American Health Assistance Foundation (Gaithersburg, MD).

ABBREVIATIONS: NMS, *N*-methylscopolamine; CHO, Chinese hamster ovary; QNB, quinuclidinyl benzilate.

equilibrium binding of muscarinic antagonists provides an alternative method for muscarinic receptor subtype-selective labeling and localization (5, 13–15).

The lack of direct labeling techniques has hampered the localization of the M4 (m4) receptor subtype in the brain. To date, mapping of the m4 receptor subtype has been limited to *in situ* hybridization studies, which demonstrate receptor gene and transcript expression but not the final distribution of receptor protein (16). Quantitative immunoprecipitation studies (17) have demonstrated the relative levels of the m4 receptor protein in various brain regions, whereas immunocytochemical studies (10) have provided a map of the distribution of the m4 receptor protein in rodent brain. Speculation regarding the functional role of the M4 (m4) receptor subtype in mammalian brain also has been hampered by the uncertain M4 localization pattern. The many similarities between the M4 (m4) and M2 (m2) receptor subtypes, including sequence homology (greater than with the m1, m3, and m5 subtypes), mechanism (attenuation of adenylate cyclase), and modulation of ionic conductance and neurotransmitter release (18–21), suggest that certain functions may be shared by these two receptor subtypes. The results presented here demonstrate that the combined use of kinetic and equilibrium binding provides a novel strategy for selective labeling of the m4 muscarinic receptor subtype in a transfected cell line and for autoradiographic M4 receptor localization studies.

Experimental Procedures

Materials. [^{3}H]NMS (79–82 Ci/mmol) was obtained from New England Nuclear (Boston MA). Dexetimide was from Research Biochemicals (Natick, MA) and atropine was from Sigma Chemical Co. (St. Louis, MO). Guanylpirenzepine was a gift from Dr. Herbert Ladinsky (Instituto De Angeli, Milan, Italy), and AF-DX 116 and pirenzepine were generously provided by Boehringer Ingelheim Pharmaceuticals (Ridgefield, CT). All tissue culture chemicals were from GIBCO-BRL (Grand Island, NY).

Cell culture. CHO-K1 cells (generously provided by Dr. Mark Brann, University of Vermont College of Medicine, Burlington, Vermont)) (11) transfected with the genes for single muscarinic receptor subtypes (m1–m5) were maintained in 75-cm^2 tissue flasks at 37° in 95% O_2/5% CO_2, in high-glucose Dulbecco's modified Eagle's medium supplemented with 10% fetal bovine serum, 100 IU/ml penicillin, 100 IU/ml streptomycin, 4 mM L-glutamine, 50 μM geneticin, and 1 mM minimal essential medium nonessential amino acids. Cells were harvested when confluence was 90–100%, by scraping of the flasks and collection of the cells in phosphate-buffered saline. Cells were lysed by homogenization with a Polytron homogenizer (Brinkman) (30 sec, at a setting of 4) in 20 mM Tris·HCl, pH 7.4, at 4°. Membranes were collected by centrifugation at 30,000 × *g* at 4° for 10 min. Final membrane resuspensions were in binding buffer at a concentration of 1–3 mg of protein/ml. Freshly prepared membranes were used for all kinetic and competition binding assays.

Ligand binding assays. Competition curves were obtained by incubating cell membranes with increasing concentrations of dexetimide (10^{-7} to 10^{-12} M), guanylpirenzepine (10^{-4} to 10^{-10} M), or pirenzepine (10^{-4} to 10^{-10} M), in the presence of 0.5 nM [^{3}H]NMS in binding buffer (50 mM phosphate buffer, pH 7.4, 1 mM $MgCl_2$). Nonspecific binding was determined in the presence of 1 μM (±)-QNB. Samples were incubated for 90 min at 25°, and labeling was terminated by rapid filtration through Whatman glass fiber filters (934-AH). Filters were washed three times with ice-cold binding buffer, dried, and counted by liquid scintillation counting in 4 ml of Cytoscint (Isolab, Irvine, CA), at an efficiency of 45%.

Kinetic studies to determine the rates of association and dissociation for [^{3}H]NMS in CHO cells were performed as described previously (15). The rates of dexetimide dissociation from m1–m5 CHO cell receptors were determined by incubating cell membranes for 30 min at 25° in 50 mM phosphate/1 mM $MgCl_2$ buffer with 10 nM dexetimide. After removal of free (unbound) dexetimide by centrifugation, cell membranes were resuspended to the original assay volume in the same buffer containing 0.5 nM [^{3}H]NMS. Aliquots of the incubation medium were removed and filtered at various times (after resuspension with the radioligand) to determine the level of unoccupied receptors. The rate of dexetimide dissociation was calculated from the percentage of sites available for [^{3}H]NMS binding, after correction for the percentage of sites occupied by [^{3}H]NMS (determined from the [^{3}H]NMS association rates).

M4 (m4)-selective labeling conditions. In membrane homogenates, selective labeling of the M4 receptor subtype was achieved as follows. Membranes (100–300 μg of protein) were incubated with 10 nM dexetimide at 25° for 30 min in 1 ml of binding buffer, to achieve ≥90% occupation of the m1, m3, m4, and m5 receptors (80% occupation of m2 receptors) (Table 1); unbound dexetimide was removed by centrifugation and membrane pellets were resuspended to the original assay volume with 0.5 nM [^{3}H]NMS, 200 nM guanylpirenzepine (93% occupation of available m1 sites and 39% occupation of available m4 sites) (Table 1), and 250 nM AF-DX 116 (83% occupation of available m2 sites and 45% occupation of available m4 sites) (Table 1) for 15 min, to allow dissociation of dexetimide from primarily the m4 receptors (see Fig. 2). [^{3}H]NMS remaining on m2 sites was removed by 10-fold dilution in 1 μM atropine solution for 5 min (see Fig. 1A). Nonspecific [^{3}H]NMS binding was measured in the presence of 1 μM (±)-QNB.

Autoradiography methods. Sagittal blocks of the left hemispheres of monkey brain were rapidly frozen in 2-methylbutane on dry ice at −30° and were subsequently stored at −80°. Sagittal sections were cut at 32 μm, thaw-mounted on gelatin-coated slides, and dried under reduced pressure at 4°. Slide-mounted sections were stored at −80° until assayed. From each sagittal hemisphere, a series of adjacent cryostat sections were processed for *in vitro* autoradiography as described above for membrane homogenates. Adjacent sections in series were quick-fixed in 70% ethanol, stained for Nissl substance, and stained with hematoxylin and eosin, to delineate architectonic boundaries and cellular profiles.

Autoradiograms were prepared by apposing the slide-mounted tissue sections, with co-placed iodine standards, to Hyperfilm (Amersham) for 6 weeks at 4°. After background subtraction, two-dimensional grayscale maps were created to allow radioactivity levels (in femtomoles/milligram) to be superimposed on the sections, as described previously (22). The film autoradiograms were scanned on a Howtech Scanmaster 3 at 400 dpi, using a transparency illuminator. The result-

TABLE 1

Dissociation constants (K_d values) for muscarinic receptor subtype-selective ligands and percentage occupancies of m1–m5 receptor subtypes expressed in CHO-K1 cells

K_d values were calculated using the Cheng-Prusoff equation (25), from computer-generated IC_{50} values for competition binding curves versus 0.5 nM [^{3}H]NMS; K_d values of m1–m5 receptors for NMS were 65, 400, 55, 49, and 106 pM, respectively (11).

Receptor subtype	Dexetimide		Guanylpirenzepine		AF-DX 116	
	K_d	Occupancy (10 nM)	K_d	Occupancy (200 nM)	K_d[a]	Occupancy (250 nM)
	nM	%	nM	%	nM	%
m1	0.28	97.3	18.0	93.0	300.0	45.5
m2	2.60	79.4	2500.0	7.4	50.0	83.3
m3	0.35	96.6	347.0	36.6	1600.0	13.5
m4	0.49	95.3	312.0	39.1	300.0	45.5
m5	0.45	95.7	175.0	53.3		

[a] From Ref. 5; values for the m1 (NB-OK1), m2 (rat heart), m3 (rat pancreas), and m4 (rat striatum) receptor subtypes were derived from [^{3}H]NMS competition binding assays.

ing tagged image format files were converted from continuous grayscale to specific activity units using the Image version 1.43 and Brain version 1.6 programs (National Institutes of Health shareware).

Data analysis. Competition curves were analyzed using the nonlinear regression analysis of the RS-1 program (BBN Software Products, Cambridge, MA). Best fit of the binding data to a one- or two-site model was determined by a partial F test of the residual sums of the squares of the respective fits. The rates of association and dissociation were calculated from linear regression analyses of the data.

The "calculated" values for the percentage occupancy of each receptor subtype at each "step" of the M4 labeling strategy were determined from the association/dissociation rates for NMS and dexetimide and from the percentage occupancy levels of the m1–m5 receptor subtypes for guanylpirenzepine, AF-DX 116, and dexetimide. Receptor occupancy levels for guanylpirenzepine, AF-DX 116, and dexetimide were determined using either published K_d values or experimentally derived K_d values, calculated from [^{3}H]NMS/ligand competition binding data by the equation percentage occupancy = [ligand]/([ligand] + K_d). Final calculated receptor occupancies were determined from (a) receptor occupancies for 10 nM dexetimide, (b) 15-min association and dissociation rates for [^{3}H]NMS and dexetimide, respectively, (c) occupancies for 200 nM guanylpirenzepine and 250 nM AF-DX 116, and (d) the 5-min [^{3}H]NMS dissociation rate.

Results

The association (Fig. 1A) and dissociation (Fig. 1B) rates for [^{3}H]NMS binding to membranes from CHO-K1 cells transfected with the m1–m5 genes are shown in Fig. 1. These data demonstrate that the rates of NMS association to the m1–m4 receptor subtypes were rapid ($t_{1/2}$, <2 min), whereas the rate of association to the m5 subtype was significantly slower ($t_{1/2}$, 6 min). The rate of NMS dissociation was significantly more rapid for the m2 receptor subtype ($t_{1/2}$, 2 min), compared with the dissociation rates for the m1, m3, m4, and m5 receptor subtypes ($t_{1/2}$, 13.4, 16.3, 17.9, and 20.5 min, respectively). This 6–7-fold difference in NMS dissociation rates between the m2 receptor subtype and the other receptor subtypes permitted the removal of [^{3}H]NMS from the m2 subtype with a short (5-min) dissociation time (80% dissociated), while leaving a significant proportion of the [^{3}H]NMS bound to the m1, m3, m4, and m5 receptor subtypes (70%, 77%, 78%, and 89% bound, respectively) (see also Ref. 15).

The rates of dexetimide dissociation from m1–m5 muscarinic receptors expressed in CHO-K1 cells are shown in Fig. 2. Greater than 90% occupancy of the m1–m5 receptors was achieved by a 15-min incubation with 10 nM dexetimide (derived from dexetimide/[^{3}H]NMS competition binding curves) (see Table 1). After removal of unbound dexetimide, the rates of dexetimide dissociation were determined from the percentage of sites available for [^{3}H]NMS binding (corrected for [^{3}H]NMS association) (Fig. 1). The results demonstrate that dexetimide dissociated very slowly from the m3 and m5 subtypes ($t_{1/2}$, 74 and 64 min, respectively), very rapidly from the m2 subtype ($t_{1/2}$, 1.4 min), and with intermediate rates from the m1 and m4 subtypes ($t_{1/2}$, 12.5 and 5.4 min, respectively). The relatively slow rates of dissociation of dexetimide from the m3 and m5 receptor subtypes provided a strategy to prevent the labeling of these receptor subtypes during short (15-min) [^{3}H]NMS incubation times.

Fig. 3 compares the competition binding curves for pirenzepine and guanylpirenzepine versus [^{3}H]NMS in m1- and m4-expressing CHO cell membranes. The curves represent the best one-site computer fits of the m1 and m4 receptor binding data for both ligands. The IC_{50} values were 89 nM and 450 nM for pirenzepine and 160 nM and 3500 nM for guanylpirenzepine for the m1 and m4 receptor subtypes, respectively. Previous studies have suggested that pirenzepine is a putative, highly selective,

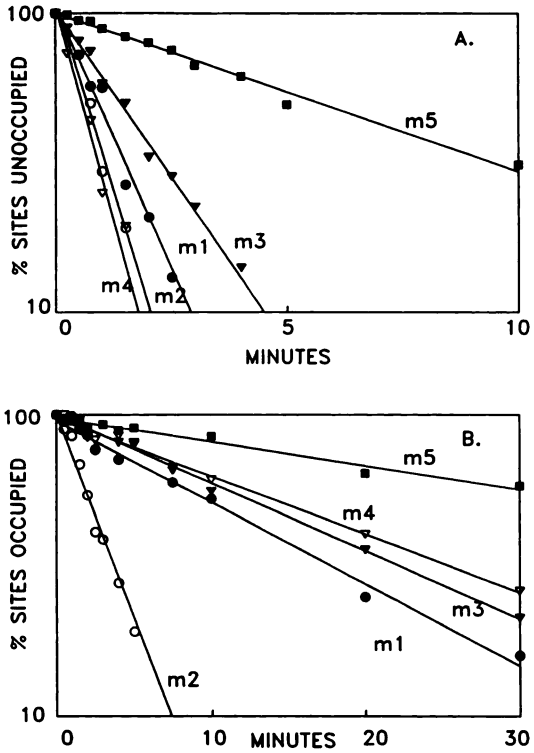

Fig. 1. Association (A) and dissociation (B) rates for [^{3}H]NMS (0.5 nM) binding to membranes from m1–m5 receptor-transfected CHO-K1 cells. Data points represent the mean of three independent experiments. *Lines*, least-squares regressions of the data points (r = 0.98). Values (mean ± standard error) for the fitted rate constants for the m1–m5 receptors are 1.39 ± 0.08 × 10^9, 1.43 ± 0.18 × 10^9, 0.90 ± 0.07 × 10^9, 2.38 ± 0.13 × 10^9, and 0.21 ± 0.07 × 10^9 M^{-1} min^{-1} for association and 0.067 ± 0.002, 0.315 ± 0.032, 0.052 ± 0.002, 0.047 ± 0.002, and 0.019 ± 0.001 min^{-1} for dissociation, respectively.

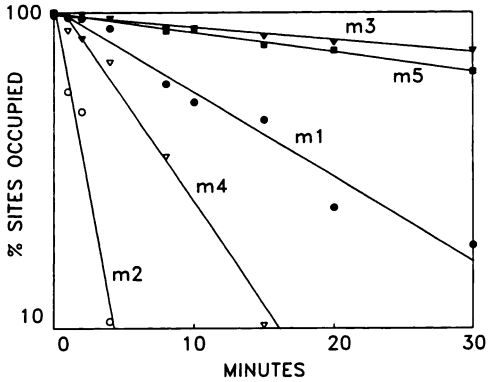

Fig. 2. Rates of dexetimide dissociation from m1–m5 receptor-expressing CHO-K1 cell membranes. After occupation of m1–m5 sites with dexetimide, the rate of dexetimide dissociation from the sites available for [^{3}H]NMS binding (0.5 nM, corrected for NMS association rates) was determined as described in Experimental Procedures. Data points are the average of two independent experiments. *Lines*, least-squares regressions of the data points (r = 0.97). Values (mean ± standard deviation) for the fitted dissociation rate constants (k_{-1}) for the m1–m5 receptors are 0.055 ± 0.008, 0.495 ± 0.121, 0.009 ± 0.002, 0.128 ± 0.013, and 0.011 ± 0.002 min^{-1}, respectively.

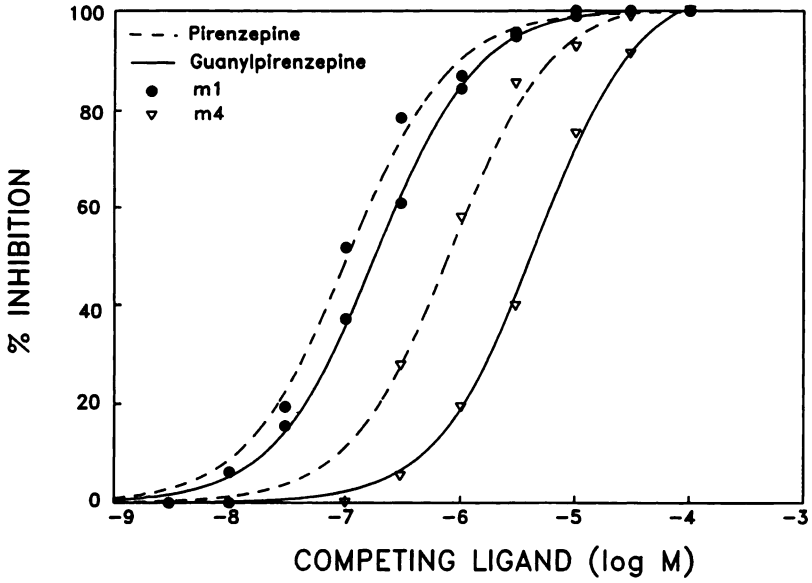

Fig. 3. Occupancy curves for pirenzepine and guanylpirenzepine with [^{3}H]NMS-labeled membranes from m1 and m4 receptor-expressing CHO-K1 cells. Data points are the means of triplicate determinations from two independent experiments (standard deviation, <2%). *Curves*, best one-site computer fit of the binding data. Curve-derived IC_{50} values for pirenzepine are 89 nM and 450 nM and for guanylpirenzepine are 160 nM and 3500 nM for the m1 and m4 receptor subtypes, respectively.

M1 receptor subtype antagonist. Although pirenzepine demonstrated higher affinities for both the m1 and m4 receptor subtypes, the m1/m4 receptor subtype selectivity of pirenzepine (5-fold) was significantly less than that of guanylpirenzepine (22-fold). The greater apparent m1 versus m4 receptor subtype selectivity profile of guanylpirenzepine, compared with pirenzepine, is also in accord with earlier reports (23, 24).

Table 1 summarizes the experimental K_d values obtained in the present study for dexetimide and guanylpirenzepine, the published K_d values for AF-DX 116 (5), and the calculated percentage occupancies, at equilibrium, of the five receptor subtypes by each of these ligands. The experimentally determined K_d values were calculated, using the equation of Cheng and Prusoff (25), from computer-generated IC_{50} values obtained from the [^{3}H]NMS competition binding assays. The K_d values for dexetimide obtained in this study were in good agreement with previously reported K_d values for [^{125}I]iododexetimide (26, 27). This finding also is consistent with previous studies demonstrating that the equilibrium K_d values (4) and kinetic binding properties (15) of muscarinic ligands are identical in clonal cell lines and in receptor subtype-specific target regions in the brain and peripheral tissues. Receptor occupancies were calculated as described in Experimental Procedures, with the indicated concentrations of ligand (200 nM guanylpirenzepine and 250 nM AF-DX 116) that were subsequently determined to be optimal for the selective labeling of the M4 receptor subtype.

Based on the relative association and dissociation rates for dexetimide and NMS at each receptor subtype and on the receptor subtype selectivity profiles assessed from competition binding data, a selective labeling strategy was devised to optimize [^{3}H]NMS labeling of the m4 receptor subtype while minimizing the labeling of the m1, m2, m3, and m5 receptor subtypes. Table 2 presents the percentage of sites available for [^{3}H]NMS binding resulting from each step of the M4 labeling strategy and the final calculated (expected) percentage occupancies for each receptor subtype. The percentage values in the left column demonstrate that, after occlusion of all receptor subtypes with 10 nM dexetimide, the relatively more rapid rates of dexetimide dissociation from the m2 and m4 receptor subtypes left ≥90% of these receptor subtypes available for

TABLE 2

Binding conditions for the selective labeling of the M4 (m4) muscarinic receptor subtype and calculated occupancies of the m1–m5 receptor subtypes

Numbers indicate the percentage of sites available with each labeling condition.

Receptor subtype	Sites available for [^{3}H]NMS binding			
	30-min dexetimide on/ 15-min dexetimide off[a]	Guanylpirenzepine (200 nM)[b]	AF-DX 116 (250 nM)[c]	5-min dissociation (final calculated)[d]
	%			
m1	61	4[e]	2	2
m2	100	93	16[e]	3[e]
m3	17[e]	11	9	7
m4	90	55	35	28
m5	23[e]	11	6	4

[a] Receptor saturation with 10 nM dexetimide (30 min), followed by 15-min dexetimide dissociation.
[b] In the presence of 200 nM guanylpirenzepine.
[c] In the presence of 250 nM AF-DX 116.
[d] Five-minute [^{3}H]NMS dissociation in the presence of 1 μM atropine.
[e] Primary receptor sites affected by the condition.

[^{3}H]NMS binding. However, 83% and 77% of the very slowly dissociating dexetimide-m3 and -m5 receptor complexes, respectively, remained occluded with dexetimide and were unavailable for radiolabeling. The intermediate rate of dexetimide dissociation from the m1 receptor subtype resulted in 61% of these sites being available for [^{3}H]NMS labeling. Inclusion of 200 nM guanylpirenzepine and 250 nM AF-DX 116 occluded the majority of the remaining m1 and m2 receptor subtypes, respectively (Table 2). Residual binding of [^{3}H]NMS to the m2 receptor subtype (16% of the total m2 sites) was reduced by a 5-min dissociation in the presence of 1 μM atropine (Table 2), improving the ratio of m4 to m2 receptor subtype labeling. The final proportions of the m1–m5 receptor subtypes labeled in CHO cell membranes with the M4 receptor subtype-selective conditions are presented in Fig. 4. The devised M4 labeling strategy resulted in an approximately 4:1 selectivity of m4 receptor subtype labeling, compared with the other receptor subtypes.

The validity of the M4 labeling strategy was further tested using *in vitro* autoradiographic methods. Previous studies (15, 28, 33, 38, 39) have demonstrated that binding affinities determined in test tube assays can be extrapolated to slide-mounted

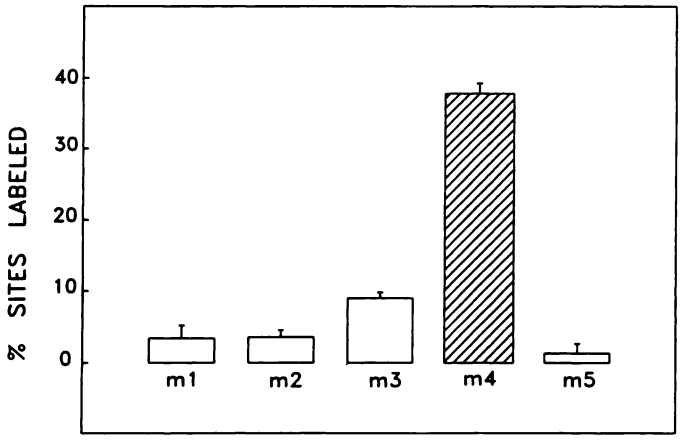

Fig. 4. Proportions of m1–m5 muscarinic receptor subtypes labeled in CHO-K1 cell membranes using the M4 (m4) receptor subtype-selective labeling conditions. *Bars*, means + standard deviations of triplicate determinations from three separate experiments.

tissue sections. *In vitro* autoradiographic localization of the M4 (m4) receptor subtype in sagittal sections of monkey brain is shown in Fig. 5. The M4 receptor subtype was widely distributed throughout the cerebral cortical mantle, overlapping previously localized M1 sites throughout most cortical fields (15). The highest densities of M4 sites in the cortex were seen over the more superficial cortical layers. Very dense M4 labeling was seen in the occipital cortex over the primary visual area (V1, area 17) and lamina 4. Highest densities of subcortical M4 receptors were found over the caudate and putamen. M4 receptors were very dense throughout all sectors of the striatum (Fig. 5) and in the medial division of the globus pallidus (data not shown). The distribution of M4 receptors was moderate in the amygdala, with a notable elevation being seen in the central nucleus (data not shown). In keeping with the dense labeling of the primary visual cortex (V1, area 17), M4 receptors were densely labeled over subcortical visual relay nuclei, including the lateral geniculate nucleus (Fig. 5, B and C) and superior colliculus (Fig. 5A). In the thalamus, M4 receptors were prevalent also in the inferior and lateral divisions of the pulvinar (Fig. 5A). This M4 receptor labeling profile is in agreement with previous *in situ* hybridization studies that demonstrated high levels of m4 mRNA in the adult rat caudate putamen and olfactory tubercle (6, 16, 28) and in the visual cortex (10, 29) and with immunocytochemical localization (10) and immunoprecipitation (17) studies.

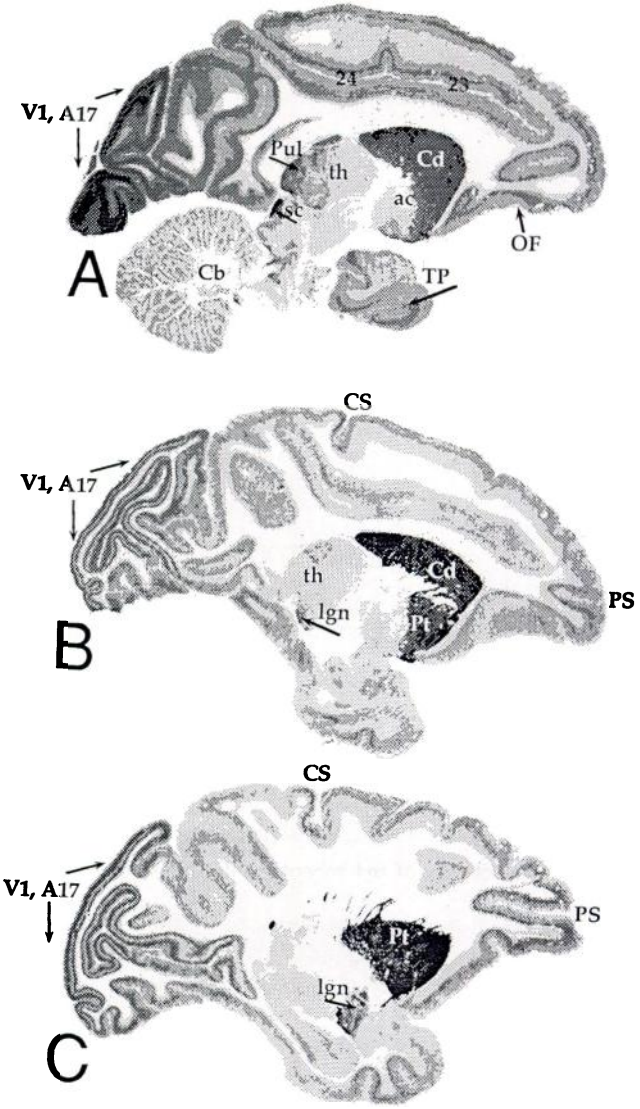

Fig. 5. Grayscale images of the M4 (m4) receptor subtype in sagittal sections (A-C, medial to lateral) of monkey brain. Computer-generated grayscale coding of the autoradiograms (*black*, highest densities; *dark gray*, intermediate densities; *light gray*, lowest densities) is shown. Note the elevated densities of the M4 receptor over the basal ganglia and primary visual area. *Cb*, cerebellum; *Cd*, caudate; *CS*, central sulcus; *lgn*, lateral geniculate nucleus; *Pt*, putamen; *sc*, superior colliculus; *th*, thalamus, *TP*, temporal lobe; *V1,A17*, primary visual area; *Pul*, pulvinar; *ac*, anterior commissure; *OF*, orbitofrontal gyrus; *23* and *24*, cingulate cortex, areas 23 and 24; *PS*, principal sulcus.

Discussion

The results presented here demonstrate that a combination of the distinct kinetic binding properties of NMS and dexetimide and the receptor subtype-selective equilibrium binding profile of guanylpirenzepine and AF-DX 116 affords differential radioligand-based labeling and autoradiographic localization of the M4 (m4) muscarinic receptor subtype. The M4 (m4) selective labeling strategy takes advantage of two distinct kinetic binding properties of muscarinic receptor subtypes. First, the very slow dissociation of most muscarinic antagonists from the m3 and m5 receptor subtypes permits the occlusion of these sites with nonradioactive antagonists that remain largely bound during subsequent removal of unbound antagonist and re-equilibration with radioligands (5, 13–15). For example, whereas the equilibrium K_d values of the five receptor subtypes for dexetimide were very similar (see Table 1), the rates of dexetimide dissociation from the m3 and m5 subtypes were approximately 10 times slower than those for the m1, m2, and m4 receptor subtypes (Fig. 2). Second, the very rapid rates of dissociation of muscarinic antagonists from the m2 receptor subtype permit the relatively selective removal of bound radioligand from this receptor subtype during short dissociation times (5, 13–15). The rate of NMS dissociation from the m2 receptor subtype was 5-fold faster than that from the m1 receptor subtype (the next fastest dissociation rate) and 18-fold faster than that from the m5 receptor subtype (the slowest dissociation rate). Thus, after the selective occlusion of the m3 and m5 receptor subtypes with dexetimide, m4-selective

[^{3}H]NMS labeling was achieved by occluding >90% and 80% of the m1 and m2 subtypes with guanylpirenzepine and AF-DX 116, respectively. The affinities of the m4 receptor for guanylpirenzepine and AF-DX 116 also resulted in 39% and 45% occupancy, respectively, of this subtype. Subsequent dissociation of [^{3}H]NMS for 5 min eliminated the majority of m2-associated [^{3}H]NMS, with minimal effects on m4-associated [^{3}H]NMS. These differential kinetic and equilibrium binding properties of muscarinic receptor subtypes have permitted the preferential labeling (4:1) of the m4 versus the m1, m2, m3, and m5 receptor subtypes.

The relative proportions of muscarinic receptor subtypes in brain regions and peripheral tissues would influence the selectivity of the described labeling conditions for the m4 receptor subtype. The labeling conditions demonstrate >10-fold selectivity for the m4 receptor subtype versus the m1, m2, and m5 receptor subtypes and 4-fold selectivity versus the m3 receptor subtype. In all brain regions examined to date (6, 10, 15, 17, 28, 36), the levels of the m1, m3, and m5 receptor subtypes exceed the level of the m4 receptor subtype by no more than 2-fold. Therefore, the relative labeling of the m4 receptor versus the m1, m3, and m5 receptors in brain should be 5:1 or greater. With the exception of the cerebellum, medulla, and pons, the m2 receptor subtype is expressed in the brain at considerably lower levels than the m4 subtype (6, 10, 15, 17, 28, 36). Selective labeling of the m4 receptor subtype should thus be achieved in most, if not all, regions of the cerebrum. In peripheral tissues with primarily a single receptor subtype (e.g., m2 in heart and m3 in glands), the described labeling conditions may not achieve the selectivity of m4 receptor labeling obtained in the brain.

The present study is the first demonstration of a selective radioligand labeling strategy for the direct autoradiographic visualization of the M4 (m4) muscarinic receptor subtype in mammalian brain. Previous attempts to determine the localization and predominance of m4 receptors in the periphery and brain have been based either on the equilibrium binding of putative "selective" antagonists or on the equilibrium binding of nonselective radioligands in the presence of nonradioactive antagonists (5, 16, 30). These approaches suffer from the lack of sufficient receptor subtype specificity, because most available muscarinic ligands demonstrate no more than 5-fold receptor subtype selectivity (12). The M4 receptor subtype has been labeled in rabbit lung by the direct binding of [^{3}H]AF-DX 384 (31). The demonstration of M4 receptors in rabbit lung with the M2/M4-selective antagonist [^{3}H]AF-DX 384 was due to the absence of the m2, m1, and m5 receptor subtypes in this organ and the predominance of the m4 receptor subtype, relative to the m3 subtype. In the brain, where the m2 receptor subtype is expressed at significantly higher levels than in the lung, neither [^{3}H]AF-DX 384 (32) nor [^{3}H]AF-DX 116 (33) would provide a practical direct approach for labeling the M4 receptor subtype.

Determination of the regional distribution of molecular subtypes of muscarinic receptors has relied on *in situ* hybridization histochemical studies (3, 6, 8, 9, 16). This approach has provided valuable information on the regional distribution and preponderance of muscarinic receptor genes and/or transcripts but does not provide information on the final distribution of receptor proteins. Recently, a correlation between the regional distributions of m4 muscarinic receptor transcripts and putative M4 receptor binding sites in rodent brain was described (28). In that study, the M4 receptor was labeled with the nonselective antagonist [^{3}H]NMS in the presence of the partially selective antagonist *p*-fluorohexahydrosiladifenidol. *p*-Fluorohexahydrosiladifenidol demonstrates only a 2-fold greater affinity for the m3 versus the m4 receptor subtype (12), resulting in significant labeling of the m3, as well as the m4, receptor subtype.

Immunocytochemical studies using receptor subtype-selective antisera have recently provided valuable information regarding the regional distribution of muscarinic receptor subtypes in the brain, thus affording high-resolution visualization of muscarinic receptor subtypes (10, 34). The combined kinetic/equilibrium mapping strategy for the M4 (m4) receptor subtype described here provides an alternative labeling approach for visualizing M4 receptors in frozen, unfixed, tissue sections. The results show that, in the cerebral cortex, M1 receptors are the most prevalent receptor subtype. This observation on the overall relative density of the cortical M1 receptors has been confirmed using subtype-selective antisera (35, 36). Quantitative immunochemical methods have shown that the M4 subtype also has high levels of expression in the cerebral cortex, comprising approximately 20% and 34% of the total density of muscarinic receptors in particular cortical fields in human (36) and rodent (10, 17) brains, respectively. In agreement with these observations, the autoradiographic localization of the M4 receptor subtype shown here is widely distributed throughout the cerebral cortical mantle, overlapping with M1 sites throughout most cortical fields (15, 37, 38). One notable difference between M1 and M4 receptors demonstrated in this study is the marked elevation of M4 binding sites over the primary visual area (V1, area 17). We have previously shown (15, 37, 38) that, in the occipital lobe, peak M2 receptor densities completely and precisely overlap with the architectonically defined primary visual area (V1, area 17). The M4 subtype has an overlapping pattern of labeling that co-registers with the M2 receptor subtype in the occipital cortex of the primate brain.

In keeping with previous localization studies of muscarinic receptor transcripts, the highest densities of subcortical M4 receptors were found over the caudate and the putamen. The dense labeling of M4 sites in subcortical visual relay nuclei, including the lateral geniculate nucleus and superior colliculus, and in the inferior and lateral subdivisions of the pulvinar within the thalamus is consistent with an association of the M4 receptor subtype with the modality of vision. These nuclei provide major projection to visual unimodal association areas (39).

The autoradiographic analysis of the M4 receptor subtype distribution demonstrated here agrees closely with previous mapping studies in rat brain, using radioligand autoradiographic and *in situ* hybridization histochemical approaches (6, 10, 16, 29, 32). Immunoprecipitation studies of m4 receptor protein using receptor subtype-specific antisera (10, 17) also are in agreement with the relative preponderance of the m4 receptor subtype in the cerebral cortex and basal ganglia. Taken together, the localization patterns in rat and primate brain suggest that M4 receptors are important targets for acetylcholine in basal ganglia circuits and in the modality of vision. Additional studies are needed to provide a comprehensive topographic map, using the combined kinetic and equilibrium

binding strategy, in primate and human brain. The *in vitro* autoradiographic results demonstrate that the combined approach is an optimal method for selectively labeling and localizing the M4 muscarinic receptor subtype.

Receptor autoradiography has demonstrated that muscarinic receptors are widely distributed throughout primate brain (15, 38). Using a combined kinetic and equilibrium binding strategy to selectively localize M1, M2, and M3 receptor subtypes (15), we have previously demonstrated that each of the receptor subtypes has a distinct localization pattern, suggesting a linkage between particular receptor subtypes and functional circuitry in the primate brain. For example, M1 receptors are prevalent throughout the paralimbic cortical areas and core limbic structures. The M2 subtype was elevated in the cerebral cortex over all primary sensory areas. In our studies, this pattern was confirmed and extended to an analysis of the putative M3 receptor subtype. Elevated densities of M3 receptors were associated with temporolimbic circuits. The results shown here for the localization of the M4 subtype in sagittal brain sections demonstrate a distinct regional binding pattern, which differs markedly from that of any of the other muscarinic receptor subtypes (for comparisons, see Ref. 15). Although the functional role of the M4 (m4) receptor subtype is not yet clear, it has been suggested that one effect of acetylcholine on this receptor subtype is to modulate the release of neurotransmitters (20, 40, 41). Consistent with this function is the recent demonstration of the enhancement of glycine release from human cerebral cortical synaptosomes by acetylcholine via the M4 receptor subtype (21). In the cerebral cortex, glycine is an obligatory factor for *N*-methyl-D-aspartate receptor excitation, acting as a glutamate modulator or coagonist to activate excitatory glutamatergic neurotransmission (42). A role for glutamate-mediated, *N*-methyl-D-aspartate receptor function in cognitive dysfunction and Alzheimer's disease is well documented (43). D-Cycloserine, a glycine receptor agonist, has been proposed for learning enhancement in animals (44) and for the treatment of cognitive memory dysfunction (45). The recent preliminary report of increased M4 (m4) receptor expression in Alzheimer's disease (36) suggests that the M4 receptor subtype may be up-regulated as a compensatory response to hypoactive glutamatergic neurotransmission. Additional studies are needed to define the relationship between M4 receptors and excitatory glutamate circuits.

References

1. Nathanson, N. M. Molecular properties of the muscarinic acetylcholine receptor. *Annu. Rev. Neurosci.* **10**:195–236 (1987).
2. Hammer, R., C. P. Berrie, N. J. M. Birdsall, A. S. V. Burgen, and E. C. Hulme. Pirenzepine distinguishes between different subclasses of muscarinic receptors. *Nature (Lond.)* **283**:90–92 (1980).
3. Bonner, T. I. The molecular basis of muscarinic receptor diversity. *Trends Neurosci.* **12**:149–151 (1989).
4. Caulfield, M. P. Muscarinic receptors: characterization, coupling and function. *Pharmacol. Ther.* **58**:319–379 (1993).
5. Waelbroeck, M., M. Tastenoy, J. Camus, and J. Christophe. Binding of selective antagonists to four muscarinic receptors (M1 to M4) in rat forebrain. *Mol. Pharmacol.* **38**:267–273 (1990).
6. Buckley, N. J., T. I. Bonner, and M. R. Brann. Localization of a family of muscarinic receptor mRNAs in rat brain. *J. Neurosci.* **8**:4646–4652 (1988).
7. Weiner, D. M., A. I. Levey, and M. R. Brann. Expression of muscarinic acetylcholine and dopamine receptor mRNAs in rat basal ganglia. *Proc. Natl. Acad. Sci. USA* **87**:7050–7054 (1990).
8. Vilaro, M. T., J. M. Palacios, and G. Mengod. Localization of m5 muscarinic receptor mRNA in rat brain examined by *in situ* hybridization histochemistry. *Neurosci. Lett.* **114**:154–159 (1990).
9. Bonner, T. I., N. J. Buckley, A. C. Young, and M. R. Brann. Identification of a family of muscarinic acetylcholine receptor genes. *Science (Washington D. C.)* **237**:527–532 (1987).
10. Levey, A. I., C. A. Kitt, W. F. Simonds, D. L. Price, and M. R. Brann. Identification and localization of muscarinic acetylcholine receptor proteins in brain with subtype-specific antibodies. *J. Neurosci.* **11**:3218–3226 (1991).
11. Buckley, N. J., T. I. Bonner, C. M. Buckley, and M. R. Brann. Antagonist binding properties of five cloned muscarinic receptors expressed in CHO-K1 cells. *Mol. Pharmacol.* **35**:469–476 (1989).
12. Dorje, F., J. Wess, G. Lambrecht, R. Tacke, E. Mutschler, and M. R. Brann. Antagonist binding profiles of five cloned human muscarinic receptor subtypes. *J. Pharmacol. Exp. Ther.* **256**:727–733 (1991).
13. Waelbroeck, M., M. Gillard, P. Robberecht, and J. Christophe. Kinetic studies of [^{3}H]*N*-methylscopolamine binding to muscarinic receptors in the rat central nervous system: evidence for the existence of three classes of binding sites. *Mol. Pharmacol.* **30**:305–314 (1986).
14. Waelbroeck, M., M. Gillard, P. Robberecht, and J. Christophe. Muscarinic receptor heterogeneity in rat central nervous system. I. Binding of four selective antagonists to three muscarinic receptor subclasses: a comparison with M2 cardiac muscarinic receptors of the C type. *Mol. Pharmacol.* **32**:91–99 (1987).
15. Flynn, D. D., and D. C. Mash. Distinct kinetic properties of *N*-[^{3}H]methylscopolamine afford differential labeling and localization of M1, M2, and M3 muscarinic receptor subtypes in primate brain. *Synapse* **14**:283–296 (1993).
16. Vilaro, M. T., K.-H. Wiederhold, J. M. Palacios, and G. Mengod. Muscarinic cholinergic receptors in the rat caudate-putamen and olfactory tubercle belong predominantly to the m4 class: *in situ* hybridization and receptor autoradiography evidence. *Neuroscience* **40**:159–167 (1991).
17. Yasuda, R. P., W. Ciesla, L. R. Flores, S. J. Wall, M. Li, M. L. Satkus, J. S. Weisstein, B. V. Spagnola, and B. B. Wolfe. Development of antisera selective for m4 and m5 muscarinic cholinergic receptors: distribution of m4 and m5 receptors in rat brain. *Mol. Pharmacol.* **43**:149–157 (1992).
18. Peralta, E. G., A. Ashkenazi, J. W. Winlsow, J. Ramachandran, and D. J. Capon. Differential regulation of PI hydrolysis and adenylyl cyclase by muscarinic receptor subtypes. *Nature (Lond.)* **334**:434–437 (1988).
19. Noda, M., M. Katayama, D. A. Brown, J. Robbins, S. J. Marsh, N. Ishizaka, K. Fukuda, N. Hoshi, S. Yokoyama, and H. Higashida. Coupling of m2 and m4 muscarinic acetylcholine receptor subtypes to Ca^{++}-dependent K channels in transformed NL308 neuroblastoma × fibroblast hybrid cells. *Proc. R. Soc. Lond. B Biol. Sci.* **251**:215–224 (1993).
20. Caulfield, M. P., and D. A. Brown. Pharmacology of the putative M4 muscarinic receptor mediating Ca-current inhibition in neuroblastoma × glioma hybrid (NG 108–15) cells. *Br. J. Pharmacol.* **104**:39–44 (1991).
21. Russo, C., M. Marchi, G. C. Andrioli, P. Cavazzani, and M. Raiteri. Enhancement of glycine release from human brain cortex synaptosomes by acetylcholine acting at m4 muscarinic receptors. *J. Pharmacol. Exp. Ther.* **266**:142–146 (1993).
22. Unnerstall, G. R., and M. J. Kuhar. Benzodiazepine receptors are coupled to a subpopulation of GABA receptors: evidence from a quantitative autoradiographic study. *J. Pharmacol. Exp. Ther.* **218**:797–804 (1982).
23. Micheletti, R., A. Schiavone, O. Angelici, P. Duranti, L. Guidici, E. Cerada, and A. Donetti. Affinity profile of the novel muscarinic antagonist, guanylpirenzepine. *Life Sci.* **47**:PL-55–PL-58 (1990).
24. Monferini, E., E. Cereda, H. Ladinsky, A. Donetti, and E. Giraldo. Guanylpirenzepine distinguishes between neuronal m1 and m4 muscarinic receptor subtypes. *J. Recept. Res.* **10**:81–92 (1990).
25. Cheng, Y., and W. H. Prusoff. Relationship between the inhibition constant (K_i) and the concentration of inhibitor which causes 50 per cent inhibition (I_{50}) of an enzymatic reaction. *Biochem. Pharmacol.* **22**:3099–3108 (1973).
26. Billings, J., B. Wolfe, A. Wilson, P. Molinoff, B. Dannals, and H. F. Kung. Characterization of I^{-125} iododexetimide: a muscarinic receptor ligand. *J. Nucl. Med.* **31**:898 (1990).
27. Laduron, P. M., M. Verwimp, and J. E. Leysen. Stereospecific *in vitro* binding of [^{3}H]dexetimide to brain muscarinic receptors. *J. Neurochem.* **32**:421–427 (1979).
28. Vilaro, M. T., G. Mengod, and J. M. Palacios. Advances and limitations of the molecular neuroanatomy of cholinergic receptors: the example of multiple muscarinic receptors. *Prog. Brain Res.* **98**:95–101 (1993).
29. Robner, S., W. Kues, V. Witzemann, and R. Schliebs. Laminar expression of m1-, m3- and m4-muscarinic cholinergic receptor genes in the developing rat visual cortex using *in situ* hybridization histochemistry: effect of monocular visual deprivation. *Int. J. Dev. Neurosci.* **11**:369–378 (1993).
30. Lazareno, S., N. L. Buckley, and F. F. Roberts. Characterization of muscarinic M4 binding sites in rabbit lung, chicken heart, and NG108–15 cells. *Mol. Pharmacol.* **38**:805–815 (1990).
31. Mak, C. W. J., E.-B. Haddad, N. J. Buckley, and P. J. Barnes. Visualization of muscarinic m4 mRNA and M4 receptor subtype in rabbit lung. *Life Sci.* **53**:1501–1508 (1993).
32. Vilaro, M. T., K.-H. Wiederhold, J. M. Palacios, and G. Mengod. Muscarinic M2-selective ligands also recognize M4 receptors in the rat brain: evidence from combined *in situ* hybridization and receptor autoradiography. *Synapse* **11**:171–183 (1992).
33. Araujo, D. M., P. A. Lapchak, W. Regenold, and R. Quirion. Characterization of [^{3}H]AF-DX 116 binding sites in the rat brain: evidence for heterogeneity of muscarinic-M_2 receptor sites. *Synapse* **4**:106–114 (1989).
34. Mrzljak, L., A. I. Levey, and P. S. Goldman-Rakic. Association of m1 and m2 muscarinic receptor proteins with asymmetric synapses in the primate

cerebral cortex: morphological evidence for cholinergic modulation of excitatory neurotransmission. *Proc. Natl. Acad. Sci. USA* **90**:5194–5198 (1993).
35. Wall, S. J., R. P. Yasuda, F. Hory, S. Flagg, B. M. Martin, E. I. Ginnis, and B. B. Wolfe. Production of antisera selective for m1 muscarinic receptors using fusion proteins: distribution of m1 receptors in rat brain. *Mol. Pharmacol.* **39**:643–649 (1991).
36. Flynn, D. D., A. I. Levey, G. Ferrari-DiLeo, and D. C. Mash. Probing the status of muscarinic receptor subtypes in Alzheimer's disease with subtype-selective antisera. *Soc. Neurosci. Abstr.* **19**:1039 (1993).
37. Mash, D. C., and L. T. Potter. Autoradiographic localization of M1 and M2 muscarine receptors in the rat brain. *Neuroscience* **19**:551–564 (1986).
38. Mash, D. C., W. F. White, and M.-M. Mesulam. Distribution of muscarinic receptor subtypes within architectonic subregions of the primate cerebral cortex. *J. Comp. Neurol.* **278**:265–274 (1988).
39. Burton, H., and E. G. Jones. The posterior thalamic region and its cortical projections in New World monkeys. *J. Comp. Neurol.* **168**:249–301 (1977).
40. McKinney, M., J. H. Miller, and P. J. Aagaard. Pharmacological characterization of the rat hippocampal muscarinic autoreceptor. *J. Pharmacol. Exp. Ther.* **264**:74–78 (1993).
41. Van Der Zee, E. A., and P. G. M. Luiten. GABAergic neurons of the rat dorsal hippocampus express muscarinic acetylcholine receptors. *Brain Res. Bull.* **32**:601–609 (1993).
42. Kemp, J. A., and P. D. Leeson. The glycine site of the NMDA receptor: five years on. *Trends Pharmacol. Sci.* **14**:20–25 (1993).
43. Maragos, W. F., J. T. Greenamyre, J. B. Penny, and A. B. Young. Glutamate dysfunction in Alzheimer's disease: an hypothesis. *Trends Neurosci.* **10**:65–68 (1987).
44. Monahan, J. B., G. E. Handelmann, W. F. Hood, and A. A. Cordi. D-Cycloserine, a positive modulator of the *N*-methyl-D-aspartate receptor, enhances performance of learning tasks in rats. *Pharmacol. Biochem. Behav.* **34**:649–653 (1989).
45. Bowen, D. M., P. T. Francis, A. W. Procter, J. V. Halliwell, D. M. A. Mann, and D. Neary. Treatment strategy for the corticocortical neuron pathology of Alzheimer's disease. *Ann. Neurol.* **32**:112 (1992).

Send reprint requests to: Donna D. Flynn, Department of Molecular and Cellular Pharmacology (R-189), University of Miami School of Medicine, P.O. Box 016189, Miami, FL 33101.